Inorg. Chem. **2006**, *45*, 7748–7757

Hybrid Inorganic–Metalorganic Compounds Containing Copper(II)-Monosubstituted Keggin Polyanions and Polymeric Copper(I) Complexes.

Leire San Felices, Pablo Vitoria,* Juan M. Gutiérrez-Zorrilla,* Luis Lezama, and Santiago Reinoso[†]

Departamento de Química Inorgánica, Facultad de Ciencia y Tecnología, Universidad del País Vasco, Apartado 644, E-48080 Bilbao, Spain

Received May 5, 2006

Four hybrid inorganic–metalorganic compounds containing copper(II)-monosubstituted Keggin polyoxotungstates, $K_3[Cu^I(4,4'\text{-bpy})]_3[SiW_{11}Cu^{II}O_{39}]\cdot 11H_2O$ (**1**), $(paraquat)_3[SiW_{11}Cu^{II}O_{39}]\cdot 6H_2O$ (**2;** paraquat = *N*,*N*′-dimethyl-4,4′-bipyridinium), $K_3[Cu^I(4,4'\text{-bpy})]_3[GeW_{11}Cu^{II}O_{39}]\cdot 11H_2O$ (**3**), and $Na_2[Cu^I(4,4'\text{-bpy})]_3[PW_{11}Cu^{II}O_{39}(H_2O)]\cdot 4H_2O$ (**4**), have been synthesized under autogenous pressure hydrothermal conditions and characterized by elemental analysis and infrared spectroscopy (FT-IR). The crystal structures of **1**, **2**, and **4** have been established by single-crystal X-ray diffraction. The crystal packings are characterized by the presence of monodimensional extended entities: either the polymeric polyanion $[SiW_{11}CuO_{39}]_n^{6n-}$ (**2**), the cationic $[Cu(4,4'\text{-bpy})]_n^{n+}$ chain (**4**), or both simultaneously as in compound **1**, where the inorganic and metalorganic sublattices are mutually perpendicular. To asses the influence of packing in the copper(I) complex structural diversity found in compounds **1** and **4**, a search in the CSD database has been performed and the resulting geometrical features have been analyzed and compared with experimental crystallographic data and DFT calculations.

Introduction

Polyoxometalates (POMs) have been attracting growing interest due to their applications in fields such as catalysis,[1] material science,[2] medicine,[3] and photochemistry.[4] As it is well-known, POMs with Keggin structure continue to have an important place at the forefront of the polyoxometalate field as a consequence of their unusual electronic versatility and structural diversity. In recent years, a series of novel hybrid compounds made of Keggin polyoxometalates associated with transition metal (TM) coordination complex cations have been described.[5] In these structures the transition metal coordination complexes provide charge compensation and also become a part of the inorganic POM framework itself[6] leading to an enrichment of the POM based hybrids chemistry. Given the importance of precise compositions and structures in all investigations focused on this class of clusters, the continuing development of synthetic methods for the systematic modification of POM systems remains very important.[7]

Under standard conditions of temperature and pressure, most of the POMs are molecular and only few examples of chains that result from the linking of transition metal monosubstituted polyoxotungstates through W−O−TM bridges have been reported.[8]

* To whom correspondence should be addressed. E-mail: pablo.vitoria@ehu.es (P.V.), juanma.zorrilla@ehu.es (J.M.G.-Z.). Fax: +34946013500.

[†] Current address: International University Bremen, School of Engineering and Science, PO Box 750 561, 28725 Bremen, Germany.

(1) (a) Misono, M. *Catal. Rev.—Sci. Eng.* **1988**, *30*, 339. (b) Ilkenhaus, T.; Herzorg, B.; Braun, T.; Schlögl, R. *J. Catal.* **1995**, *153*, 275. (c) Belanger, R.; Moffat, J. B. *J. Catal.* **1995**, *152*, 171. (d) Corma, A. *Chem. Rev.* **1995**, *95*, 559. (e) Hill, C. L.; Prosser-Mccartha, M. *Coord. Chem. Rev.* **1995**, *143*, 407. (f) Kozhevnikov, I. V. *Catal. Rev.—Sci. Eng.* **1995**, *37*, 311. (g) Neumann, R. *Prog. Inorg. Chem.* **1998**, *47*, 317. (h) Okuhara, T.; Mizuno, N.; Misono, M. *Adv. Catal.* **1996**, *41*, 113. (i) Kuznetsova, L. I.; Maksimov, G. M.; Likholobov, V. A. *Kinet. Catal.* **1999**, *40*, 622. (j) Misono, M. *Chem. Commun.* **2001**, 1141. (k) Khenkin, A. M.; Weiner, L.; Wang, Y.; Neumann, R. *J. Am. Chem. Soc.* **2001**, *123*, 8531. (l) Kozhevnikov, I. V. *Catalysts for Fine Chemicals; Vol 2. Catalysis by Polyoxometalates*; Wiley: Chichester, U.K., 2002. (m) Kozhevnikov, I. V. *Innovations Pharm. Technol.* **2003**, *3*, 96. (n) Okun, N. M.; Anderson, T. M.; Hardcastle, K. I.; Hill, C. L. *Inorg. Chem.* **2003**, *42*, 6610. (o) Kiricsi, I., Ed. *Appl. Catal., A: Gen.* **2003**, *256* (1), special thematic issue. (p) Hill, C. L. *Angew. Chem., Int. Ed.* **2004**, *43*, 402. (q) Liu H.; Iglesia, E. *J. Catal.* **2004**, *223*, 161. (r) Stahl, S. S. *Angew. Chem., Int. Ed.* **2004**, *43*, 3400. (s) Kholdeeva, O. A.; Vanina, M. P.; Timofeeva, N. N.; Maksimovskaya, R. I.; Trubitsina, T. A.; Melgunov, M. S.; Burgina, E. B.; Mrowiec-Bialon, J.; Jarzebski, A. B.; Hill, C. L. *J. Catal.* **2004**, *226*, 363. (t) Won, B. K.; Voitl, T.; Rodríguez-Rivera, G. J.; Dumesic, J. A. *Science* **2004**, *305*, 1280.

10.1021/ic060762g CCC: $33.50
Published on Web 08/18/2006

Currently, we are exploring the applicability of Keggin POMs and TM cationic complexes in the preparation of new attractive hybrid inorganic−metalorganic compounds.[9]

The recent introduction of hydrothermal synthetic methods in the field of POMs has led to a plethora of extended materials, which are difficult to isolate under standard conditions.[10] Thus, we have explored the hydrothermal route for the preparation of such extended solid-state materials based on Keggin POMs starting from simple building blocks. Here we report the synthesis, chemical and spectroscopic characterization, and X-ray crystal structure determination of $K_3[Cu^I(4,4'\text{-bpy})]_3[SiW_{11}Cu^{II}O_{39}]\cdot 11H_2O$ (**1**), $(paraquat)_3[SiW_{11}Cu^{II}O_{39}]\cdot 6H_2O$ (**2**), $K_3[Cu^I(4,4'\text{-bpy})]_3[GeW_{11}Cu^{II}O_{39}]\cdot 11H_2O$ (**3**), and $Na_2[Cu^I(4,4'\text{-bpy})]_3[PW_{11}Cu^{II}O_{39}(H_2O)]\cdot 4H_2O$ (**4**). To assess the influence of the crystal packing in the copper(I) complex cation geometries, a search in the CSD database has been performed and the resulting geometrical features have been analyzed through continuous shape measures (CSM) and compared with crystallographic data and DFT calculations.

Experimental Section

Materials and Methods. The compound $K_8[\alpha\text{-}SiW_{11}O_{39}]\cdot 13H_2O$ was prepared according to the procedure described in the literature.[11] The same synthetic procedure was used to obtain $K_8[\alpha\text{-}GeW_{11}O_{39}]\cdot 9H_2O$, using GeO_2 instead of Na_2SiO_3. All other chemicals were obtained from commercial sources and used without further purification. Infrared spectra for solid samples were obtained as KBr pellets on a Mattson 1000 FTIR spectrometer. EPR powder spectra were recorded on a Bruker ESP300 spectrometer (magnetic field calibration, NMR probe; determination of the frequency inside the cavity, Hewlett-Packard5352B microwave frequency counter). Carbon, nitrogen, and hydrogen were determined by organic microanalysis on a LECO CHNS-932 analyzer.

Synthesis of $K_3[Cu^I(4,4'\text{-bpy})]_3[SiW_{11}Cu^{II}O_{39}]\cdot 11H_2O$ (1) and $(paraquat)_3[SiW_{11}Cu^{II}O_{39}]\cdot 6H_2O$ (2). A mixture of $K_8[\alpha\text{-}SiW_{11}O_{39}]\cdot 13H_2O$ (644 mg, 0.20 mmol), $CuCl_2\cdot 2H_2O$ (108 mg, 0.63 mmol), oxalic acid dihydrate (25 mg, 0.20 mmol), and 4,4′-bipyridine (64 mg, 0.41 mmol) was stirred for 30 min in a mixture of methanol (10 mL) and 1 M acetic acid/potassium acetate buffer solution (25 mL) and then transferred to a 40 mL Teflon-lined stainless steel reactor. The solution was heated under autogenous pressure at 170 °C for 72 h. After the solution was slowly cooled to room temperature at a rate of 6 °C/h, a mixture of prismatic crystals of compounds **1** (yellow) and **2** (colorless) and red crystals of cuprite (Cu_2O)[12] were obtained. Visual examinations under an optical microscope allowed us to separate crystals suitable for single-crystal X-ray diffraction studies and a sufficient amount to perform physical characterizations. The crystals were filtered out, washed with abundant distilled water, and dried in air. Anal. Calcd (found) for $C_{30}H_{48}Cu_4K_3N_6O_{50}SiW_{11}$ (**1**): C, 9.70 (9.83); H, 1.30 (1.37); N, 2.26 (2.16). Calcd (found) for $C_{30}H_{47}CuKN_5O_{45}SiW_{11}$ (**2**): C, 10.75 (10.38); H, 1.41 (1.10); N, 2.09 (2.03).

Synthesis of $K_3[Cu^I(4,4'\text{-bpy})]_3[GeW_{11}Cu^{II}O_{39}]\cdot 11H_2O$ (3). Method A. A mixture of $K_8[\alpha\text{-}GeW_{11}O_{39}]\cdot 9H_2O$ (657 mg, 0.21 mmol), $CuCl_2\cdot 2H_2O$ (108 mg, 0.63 mmol), oxalic acid dihydrate (25 mg, 0.20 mmol), and 4,4′-bipyridine (64 mg, 0.41 mmol) was stirred for 30 min in a mixture of methanol (10 mL) and 1 M acetic

(2) (a) Gómez-García, C. J.; Coronado, E.; Ouahab, L. *Angew. Chem., Int. Ed. Engl.* **1992**, *31*, 240. (b) Coronado, E.; Gómez-García, C. J. *Comments Inorg. Chem.* **1995**, *17*, 255. (c) Clemente-Juan, J. M.; Coronado, E. *Coord. Chem. Rev.* **1999**, *193*−*195*, 361. (d) Ouahab, L. *Chem. Mater.* **1997**, *9*, 1909; *Coord. Chem. Rev.* **1998**, *178*−*180*, 1501. (e) Coronado, E.; Galán-Mascarós, J. R.; Giménez-Sáiz, C.; Gómez-García, C. J. *Adv. Mater. Opt. Electron.* **1998**, *8*, 61. (f) Kurth, D. G.; Lehmann, P.; Volmer, D.; Muller, A.; Schwahn, D. *J. Chem. Soc., Dalton Trans.* **2000**, 3989. (g) Clemente-León, M.; Coronado, E.; Delhaes, P.; Gómez-García, C. J.; Mingolaud, C. *Adv. Mater.* **2001**, *13*, 574. (h) Clemente-León, M.; Coronado, E.; Gómez-García, C. J.; Martínez-Ferrero, E. *J. Cluster Sci.* **2002**, *13*, 381. (i) Clemente-Juan, J. M.; Coronado, E.; Forment-Aliaga, A.; Galán-Mascarós, J. R.; Giménez-Sáiz, C.; Gómez-García, C. J. *Inorg. Chem.* **2004**, *43*, 2689. (j) Forment-Aliaga, A.; Coronado, E.; Feliz, M.; Gaita-Ariño, A.; Llusar, R.; Romero, F. M. *Inorg. Chem.* **2004**, *43*, 8019. (k) Casañ-Pastor, N.; Gómez-Romero P. *Front. Biosci.* **2004**, *9*, 1759.

(3) (a) Michelon, M.; Hervé, M.; Hervé, G. *Biochim. Biophys. Acta* **1987**, *916*, 402. (b) Yamase, T.; Fujita, M.; Fukushima, K. *Inorg. Chim. Acta* **1988**, *151*, 15. (c) Chottard, G.; Hill, C. L.; Weeks, M. S.; Schinazi, R. F. *J. Med. Chem.* **1990**, *33*, 2767. (d) Inouye, Y.; Tale, Y.; Tokutake, Y.; Yoshida, T.; Yamamoto, A.; Yamase, T.; Nakamura, S. *Chem. Pharm. Bull.* **1990**, *38*, 285. (e) Barnard, D. L.; Hill, C. L.; Gage, T.; Matheson, J. E.; Huffman, J. H.; Sidwell, R.; Otto, M. I.; Schinazi, R. F. *Antiviral Res.* **1997**, *34*, 27. (f) Fukuda, N.; Yamase, T.; Tajima, Y. *Biol. Pharm. Bull.* **1999**, *22*, 463. (g) Rhule, J. T.; Hill, C. L.; Zheng, Z.; Schinazi, R. F. *Top. Biol. Inorg. Chem.* **1999**, *2*, 117. (h) Botto, I. M.; Barrio, D. A.; Egusquiza, M. G.; Cabello, C. I.; Cortizo, A. M.; Etcheverry, S. B. *Met. Ions Biol. Med.* **2002**, *7*, 159. (i) Wang, X.; Liu, J.; Li, J.; Yang Y.; Liu, J.; Li, B.; Pope, M. T. *J. Inorg. Biochem.* **2003**, *94*, 279. (j) Wang, X.; Liu, J.; Pope, M. T. J. *Dalton Trans.* **2003**, 957.

(4) (a) Hou, Y.; Hill, C. L. *New J. Chem.* **1992**, *16*, 909. (b) Yamase, T. *Mol. Eng.* **1993**, *3*, 241. (c) Papaconstantinou, E. *Trends Photochem. Photobiol.* **1994**, *3*, 139. (d) Gómez-Romero, P.; Casañ-Pastor, N. *J. Phys. Chem.* **1996**, *100*, 12448. (c) Athanasios, M.; Hiskia, A.; Androulaki, E.; Dimitikali, D.; Papaconstantinou, E. *Phys. Chem. Chem. Phys.* **1999**, *1*, 437. (e) Yamase, T.; Prokop P. V. *Angew. Chem., Int. Ed.* **2002**, *41*, 466. (f) Ruether, T.; Hultgren, V. M.; Timko, B. P.; Bond, A. M.; Jackson, W. R.; Wedd, A. G. *J. Am. Chem. Soc.* **2003**, *125*, 10133. (g) Hill, C. L. In *Comprehensive Coordination Chemistry II*; McCleverty, J. A., Meyer, T. J., Eds.; Elsevier Ltd.: Oxford, U.K., 2004; Vol. 4.

(5) (a) Xu, Y.; Zhang, K.-L.; Zhang, Y.; You, X.-Z.; Xu, J.-Q. *Chem. Commun.* **2000**, 153. (b) Niu, J.; Wu, Q.; Wang, J. *J. Chem. Soc., Dalton Trans.* **2002**, 2512. (c) Niu, J.; Wang, Z.; Wang, J. *Inorg. Chem. Commun.* **2003**, *6*, 1272. (d) Niu, J.; Wei, M.; Wang, J.; Dang, D. *J. Mol. Struct.* **2003**, *655*, 171. (e) Dolbecq, A.; Mialane, P.; Lisnard, L.; Marrot, J.; Sécheresse, F. *Chem.*−*Eur. J.* **2003**, *9*, 2914.

(6) Hu, C.; Wang, Y.; Li, Y.; Wang, E. *Chem. J. Internet* **2001**, *3*, 22 (http://web.chemistrymag.org/cji/2001/036022re.htm) and references therein.

(7) Anderson T. M.; Hardcastle, K. I.; Okun, N.; Hill, C. L. *Inorg. Chem.* **2001**, *40*, 6418.

(8) (a) Galán-Mascarós, J. R.; Giménez-Saiz, C.; Triki, S.; Gómez-García, C. J.; Coronado, E.; Ouahab, L. *Angew. Chem., Int. Ed.* **1995**, *34*, 1460. (b) Coronado, E.; Galán-Mascarós, J. R.; Giménez-Saiz, C.; Gómez-García, C. J.; Triki, S. *J. Am. Chem. Soc.* **1998**, *120*, 4671. (c) Evans, H. T.; Weakley, T. J. R.; Jameson, G. B. *J. Chem. Soc., Dalton Trans.* **1996**, 2537. (d) Yan, B.; Xu, Y.; Bu, X.; Goh, N. K.; Chia, L. S.; Stucky, G. D. *J. Chem. Soc., Dalton Trans.* **2001**, 2009. (e) Nyman, M.; Bonhomme, F.; Alam, T. M.; Rodriguez, M. A.; Cherry, B. R.; Krumhansl, J. L.; Nenoff, T. M.; Sattler, A. M. *Science* **2002**, *297*, 996. (f) Lisnard, L.; Dolbecq, A.; Mialane, P.; Marrot, J.; Sécheresse, F. *Inorg. Chim. Acta* **2004**, *357*, 845.

(9) (a) Reinoso, S.; Vitoria, P.; Lezama, L.; Luque, A.; Gutiérrez-Zorrilla, J. M. *Inorg. Chem.* **2003**, *42*, 3709. (b) Reinoso, S.; Vitoria, P.; Gutiérrez-Zorrilla, J. M.; Lezama, L.; San Felices, L.; Beitia, J. I. *Inorg. Chem.* **2005**, *44*, 9731. (c) San Felices, L.; Vitoria, P.; Gutiérrez-Zorrilla, J. M.; Reinoso, S.; Etxebarria, J.; Lezama, L. *Chem.*−*Eur. J.* **2004**, *10*, 5138. (d) Reinoso, S.; Vitoria, P.; San Felices, L.; Lezama, L.; Gutiérrez-Zorrilla, J. M. *Inorg. Chem.* **2006**, *45*, 108.

(10) (a) Lisnard, L.; Dolbecq, A.; Mialane, P.; Marrot, J.; Codjovi, E.; Sécheresse, F. *Dalton Trans.* **2005**, 3913. (b) Ritchie, C.; Burkholder, E.; Kögerler, P.; Cronin, P. *Dalton Trans.* **2006**, 1712. (c) Ren, Y.-P.; Kong, X.-Y.; Hu, X.-Y.; Sun, M.; Long, L.-S.; Huang, R.-B.; Zheng, L.-S *Inorg. Chem.* **2006**, *45*, 4016. (d) Cronin, L. *Annu. Rep. Prog. Chem., Sect. A: Inorg. Chem.* **2004**, *100*, 323.

(11) Tézé, A.; Hervé G. *J. Inorg. Nucl. Chem.* **1977**, *39*, 999.

(12) Single-crystal X-ray diffraction: cubic crystal system; $Pn\bar{3}m$ space group; $a = 4.2677(7)$ Å; $V = 77.73(2)$ Å^3. These data are in very good agreement with data in the following: Restori, R.; Schwarzenbach, D. *Acta Crystallogr.* **1986**, *B42*, 201.

Table 1. Crystallographic Data for Compounds **1**−**4**

	1	**2**	**3**	**4**
formula	$C_{30}H_{48}Cu_4K_3N_6O_{50}SiW_{11}$	$C_{30}H_{47}CuKN_5O_{45}SiW_{11}$	$C_{30}H_{48}Cu_4K_3N_6O_{50}GeW_{11}$	$C_{60}H_{56}Cu_8N_{12}Na_4O_{88}P_2W_{22}$
fw	3714.52	3350.67	3759.04	7059.87
cryst system	orthorhombic	triclinic	orthorhombic	monoclinic
space group	*Pbcb*	$P\bar{1}$	*Pbcb*	$P2_1/a$
a (Å)	10.9722(4)	10.897(1)	11.049(4)	21.253(2)
b (Å)	21.5961(7)	13.103(1)	21.528(8)	21.792(1)
c (Å)	28.0216(8)	21.442(1)	28.182(8)	27.105(1)
α (deg)	90	87.227(6)	90	90
β (deg)	90	85.004(5)	90	101.790(6)
γ (deg)	90	84.328(6)	90	90
V (Å^3)	6639.9(4)	3033.0(2)	6704(4)	12288(1)
D_{cal} (g·cm^{-3})	*3.716*	*3.669*	*3.724*	*3.816*
Z	4	2	4	4
μ (mm^{-1})	20.536	21.304	20.761	21.997
collcd reflcns	42 394	20 408		66 667
unique reflcns (R_{int})	6531 (0.041)	11 678 (0.054)		21 555 (0.088)
obsd reflcns $I > 2\sigma(I)$	5109	6032		7074
params	*347*	*443*		*947*
S	1.309	0.813		0.807
$R(F_o)^a$ (obsd reflcns)	0.078	0.045		0.069
$wR(F_o^2)^a$ (all reflcns)	0.152	0.082		0.139
χ^2			2.96	
R_p			7.68	
R_{wp}			10.8	

^{a} $R(F_o) = \Sigma||F_o| - |F_c||/\Sigma|F_o|$; $wR(F_o^2) = \{\Sigma[w(F_o^2 - F_c^2)^2]/\Sigma[w(F_o^2)^2]\}^{1/2}$.

Scheme 1

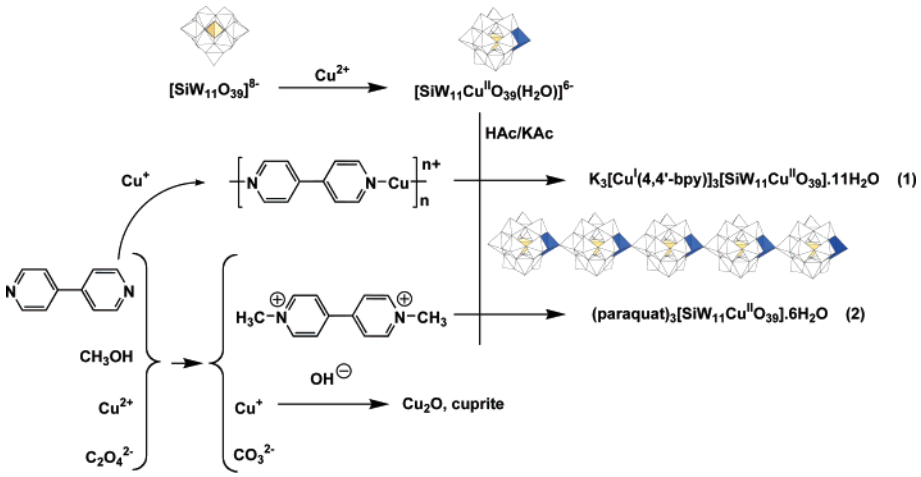

acid/potassium acetate buffer solution (25 mL) and then transferred to a 40 mL Teflon-lined stainless steel reactor. The solution was heated under autogenous pressure at 170 °C for 72 h. After the solution was slowly cooled to room temperature at a rate of 6 °C/h, yellow prismatic crystals of compound **3** were obtained (yield: 237 mg, 40% based on Cu).

Method B. A mixture of GeO_2 (28 mg, 0.27 mmol), $Na_2WO_4 \cdot 2H_2O$ (720 mg, 2.2 mmol), $CuCl_2 \cdot 2H_2O$ (108 mg, 0.63 mmol), oxalic acid dihydrate (25 mg, 0.20 mmol), and 4,4′-bipyridine (64 mg, 0.41 mmol) was stirred for 30 min in a mixture of methanol (10 mL) and 1 M acetic acid/potassium acetate buffer solution (25 mL) and then transferred to a 40 mL Teflon-lined stainless steel reactor. The solution was heated under autogenous pressure at 170 °C for 72 h. After the solution was slowly cooled to room temperature at the rate of 6 °C/h, yellow prismatic crystals of compound **3** were obtained. The crystals were filtered out, washed with abundant distilled water, and dried in air (yield: 450 mg, 72% based on Cu). Anal. Calcd (found) for $C_{30}H_{48}Cu_4K_3N_6O_{50}GeW_{11}$ (**3**): C, 9.59 (9.37); H, 1.29 (1.18); N, 2.24 (2.21).

Synthesis of $Na_2[Cu^I(4,4'\text{-bpy})]_3[PW_{11}Cu^{II}O_{39}(H_2O)] \cdot 4H_2O$ (4). Due to the very low solubility in water of the potassium salt of the monolacunary tungstophosphate, $K_7[\alpha\text{-}PW_{11}O_{39}]$, the synthetic procedure was as follows: a mixture of $Na_2HPO_4 \cdot 2H_2O$ (28 mg, 0.16 mmol), $Na_2WO_4 \cdot 2H_2O$ (528 mg, 1.6 mmol), $Cu(CH_3CO_2)_2 \cdot H_2O$ (80 mg, 0.4 mmol), and 4,4′-bipyridine (125 mg, 0.8 mmol) was stirred for 30 min in methanol (10 mL) and 1 M acetic acid/sodium acetate buffer solution (25 mL) and then transferred to a 40 mL Teflon-lined stainless steel reactor. The solution was heated under autogenous pressure at 170 °C for 144 h. After the solution was slowly cooled to room temperature at the rate of 3 °C/h, yellow prismatic crystals of compound **4** were obtained. The crystals were filtered out, washed with abundant distilled water, and dried in air (yield: 494 mg, 70% based on Cu). Anal. Calcd (found) for $C_{60}H_{56}Cu_8N_{12}$ $Na_4O_{88}P_2W_{22}$ (**4**): C, 10.20 (10.28); H, 0.80 (0.73); N, 2.38 (2.29).

X-ray Data Collection and Structure Determination. Experimental details and crystal data for all four compounds are given in Table 1. Data for the single-crystal X-ray studies of compounds **1**, **2**, and **4** and cuprite were collected at room temperature on a Xcalibur diffractometer (graphite-monochromated Mo Kα radiation, $\lambda = 0.710\ 73$ Å) fitted with a Sapphire CCD detector. Data frames were processed (unit cell determination, intensity data integration,

Table 2. Important Assignments in the IR Spectra of POMs in Compounds **1**−**4**, Compared with the DFT-Optimized $[XW_{11}O_{39}Cu^{II}(H_2O)]^{n-}$ and $[XW_{12}O_{40}]^{n-}$ Polyanions

	Si				Ge			P		
assgnt	**1**	**2**	$SiW_{11}Cu^a$	SiW_{12}^a	**3**	$GeW_{11}Cu^a$	GeW_{12}^a	**4**	$PW_{11}Cu^a$	PW_{12}^a
$\nu_{as}(X-O_c)+\nu_{as}(W-O_t)$ antisym	1012 w	1012 w	992 w	1007 w	946 sh	948 vw	982 sh	1103 m	1084 w	1075 w
	1002 w	1000 w	977 w			934 sh		1060 m	1052 w	
$\nu_{as}(W-O_t)$	948 m	951 m	917 m	962 m	928 sh	912 vs	961 m	954 m	938 m	978 m
$\nu_{as}(X-O_c)+\nu_{as}(W-O_t)$ sym	901 vs	899 vs	888 vs	930 vs			912 vs	885 m	891 m	918 m
$\nu_{as}(W-O_v-W)$	867 sh	871 sh	871 sh	899 m	881 vs	877 vs		811 vs	832 vs	848 vs
$\nu_{as}(X-O_c)+\nu_{as}(W-O_b-W)+\nu_{as}(Cu-O)^b$					815 vs	810 vs	831 m			
					790 sh	788 m	803 m			
					730 sh	732 w				
$\nu_{as}(W-O_a-W)+\nu_{as}(Cu-O)^b$	798 vs	797 vs	813 vs	829 vs				752 sh	752 w	
	746 m	746 m	746 m							
$\nu_{as}(Cu-O)$	696 m	692 m	696 m		673 w	682 w		706 w	708 w	
$\delta(W-O_a-W)+\delta(X-O_c)$	541 w	538 w	541 w	556 w	530 w	530 sh	536 w	602 w		576 w
	528 w	526 sh	528 w	532 w	513 sh	514 w	527 w	518 sh		529 w
$\delta(W-O_b-W)+\delta(X-O_c)$					466 w	468 w	475 w			
						447 w				
						431 w				
						420 w				
$\delta(W-O_b-W)$	428 w	499 w	428 w	416 w			404 w	442 w	410 w	420 w

[a] Optimized. [b] Only in Cu-monosubtituted POM.

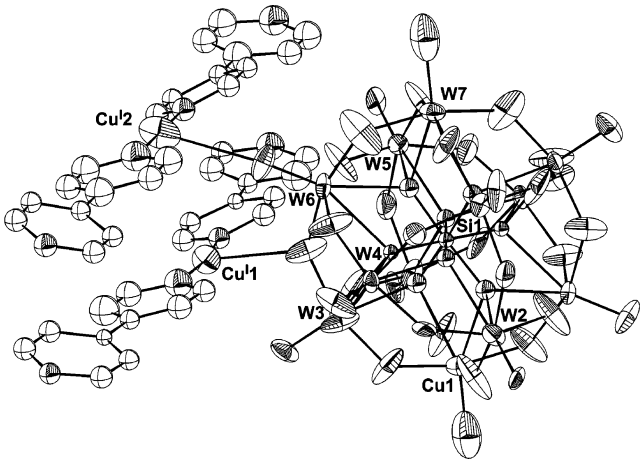

Figure 1. ORTEP view of the compound $[Cu^I(4,4'\text{-bpy})]_3[SiW_{11}Cu^{II}O_{39}]$ (**1**) with atom labeling.

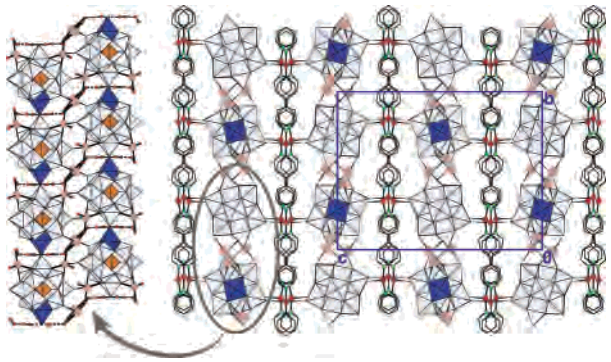

Figure 2. Crystal packing of compound **1** viewed along the [100] direction with a detailed view of the linking through K cations and water molecules of antiparallel chains to give a 2D arrangement.

correction for Lorentz and polarization effects, and analytical absorption correction) using the CrysAlis software package.[13] Neutral atom scattering factors and anomalous dispersion factors were taken from the literature.[14] The structures were solved using a combination of Patterson and direct methods (DIRDIF-99)[15] and refined by full-matrix least-squares analysis with the SHELXL-97 program.[16] Thermal vibrations were treated anisotropically for heavy atoms.

The copper atom in the polyanions was disordered over two tungsten positions in compounds **1** and **2** and over five positions in the case of compound **4**. In all cases their population parameters were refined without restrictions, resulting in the expected number of one copper ion/Keggin subunit. Hydrogen atoms of the bipyridine ligands and paraquat cations were placed in calculated positions and refined with a riding model using default SHELXL parameters. All crystallographic calculations were performed using the WinGX software package.[17] The final geometrical calculations were carried out with the PLATON program.[18]

Crystals of compound **3** were of insufficient quality to be studied by X-ray single-crystal diffraction, and powder X-ray diffraction was performed to obtain structural information. The X-ray powder diffraction pattern was recorded on a Phillips PW1470 X′Pert diffractometer equipped with graphite-monochromated Cu $K\alpha_1$ radiation. A scan was performed in the $5 < 2\theta < 40°$ range with increments of 0.02° and a fixed counting time of 20 s. Indexation of the diffraction profile and refinement of the cell parameters were performed with the program Fullprof[19] (pattern-matching analysis) on the basis of the space group and the cell parameters found for the isostructural compound **1**.

Computational Details. All density functional theory (DFT) calculations were carried out with the Gaussian 03 program[20] running on a GNU/Linux cluster. The optimization procedure for the $[SiW_{11}O_{39}Cu^{II}(H_2O)]^{6-}$ and $[SiW_{12}O_{40}]^{4-}$ polyanions has been previously reported,[21] and the same functional (B3LYP[22]) and basis sets were used for the optimization of the germanium and phosphorus analogues. Infrared spectra were calculated on the

(13) Oxford Diffraction: *CrysAlis CCD and RED*, version 1.71; Oxford Diffraction, Ltd.: Oxford, U.K., 2003.

(14) *International Tables for X-ray Crystallography*; Kynoch Press: Birmingham, U.K., 1974; Vol. IV.

(15) Beurkens, P. T.; Beurkens, G.; de Gelder, R.; García-Granda, S.; Gould, R. O.; Israel; R.; Smits, J. M. M. *The DIRDIF-99 Program System*; Crystallography Laboratory, University of Nijmegen: Nijmegen, The Netherlands, 1999.

(16) Sheldrick, G. M. *SHELXL97*; University of Göttingen: Göttingen, Germany, 1999.

(17) Farrugia, L. *J. Appl. Crystallogr.* **1999**, *32*, 837.

(18) Spek, A. L. *PLATON*; Utrecht University: Utrecht, The Netherlands, 2005.

(19) Rodríguez-Carvajal, J. *Physica B* **1993**, *152*, 55.

Table 3. Ranges of M−O Bond Distances in Compounds **1**, **2**, and **4** Compared with the Optimized $[XW_{11}O_{39}Cu^{II}(H_2O)]^{n-}$ and $[XW_{12}O_{40}]^{n-}$ Polyanions

	Si				P			
					4			
param	**1**	**2**	$[SiW_{11}O_{39}Cu(H_2O)]^{6-}$ [a]	$[SiW_{12}O_{40}]^{4-}$ [a]	subunit 1	subunit 2	$[PW_{11}O_{39}Cu(H_2O)]^{5-}$ [a]	$[PW_{12}O_{40}]^{3-}$ [a]
W−O_c [b]	2.26−2.47	2.28−2.40	2.33−2.44	2.393	2.39−2.45	2.38−2.46	2.42−2.52	2.472
W−O_b [b]	1.83−1.95	1.84−1.99	1.83−2.03	1.923, 1.935	1.80−1.98	1.85−1.97	1.81−2.02	1.924, 1.931
W−O_t [b]	1.65−1.71	1.67−1.74	1.76−1.77	1.740	1.66−1.77	1.66−1.74	1.75−1.76	1.730
X−O_c	1.55−1.68	1.61−1.64	1.64−1.66	1.650	1.52−1.59	1.52−1.57	1.57−1.59	1.574
Cu−O_c	2.40−2.44	2.35−2.36	2.319		2.39−2.50	2.38−2.50	2.361	
Cu−O_b	1.90−1.96	1.92−1.97	2.011, 2017		1.83−2.01	1.81−2.02	2.009	
Cu−O_t	1.90−2.06	1.99−2.03	2.287		1.62−1.82	1.69−1.82	2.246	
Cu···X	3.48−3.54	3.51−3.52	3.377		3.51−3.56	3.52−3.60	3.405	
X···$W_{trans-Cu}$	3.48−3.54	3.51−3.52	3.589		3.54−3.58	3.52−3.60	3.617	
W···X	3.51−3.54	3.52−3.56	3.56−3.64	3.588	3.53−3.56	3.51−3.56	3.59−3.67	3.619
Cu···W_{trans}	7.01	7.03	6.963		7.07−7.13	7.08−7.14	7.020	
W···W_{trans}	7.02−7.05	7.04−7.07	7.15−7.21	7.173	7.09−7.12	7.07−7.11	7.21−7.27	7.236
O_{Cu}···O_{Wtrans}	10.97	10.90	10.710		10.42−10.65	10.47−10.63	10.787	
O···O_{trans}	10.40−10.43	10.34−10.44	10.62−10.69	10.594	10.42−10.50	10.41−10.44	10.67−10.7 3	10.648

[a] Optimized. [b] O_c: oxygen atoms belonging to the central SiO_4 tetrahedron. O_b: bridging oxygen atoms between MO_6 octahedra. O_t: terminal oxygen atoms.

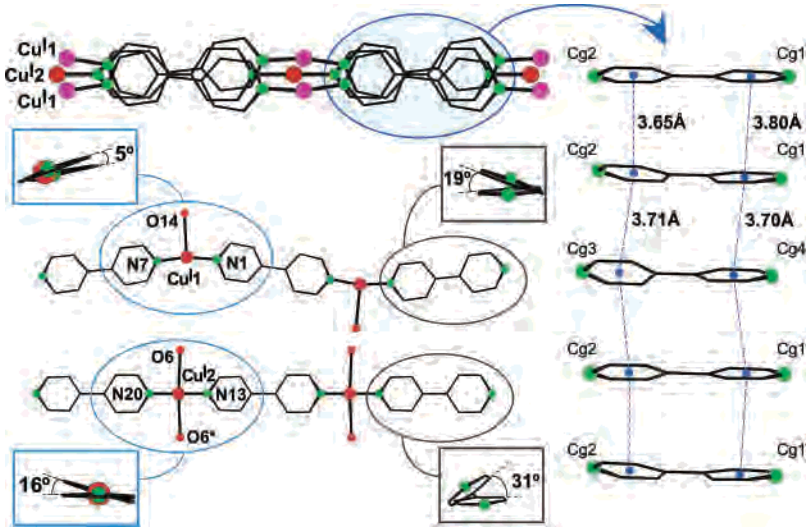

Figure 3. Metalorganic chains in compound **1** with coordination spheres of copper(I) ions and torsion angles between aromatic rings (bottom). Shown are details of $\pi-\pi$ interactions along the stacking direction indicating distances between ring centroids [aromatic ring labels: Cg1, N1−C6; Cg2, N7−C12; Cg3, N13−C16; Cg4, C17−N20] (right).

optimized geometry of the six mentioned species. The infrared active vibrational frequencies were identified using the GaussviewW 3.0 program,[23] which provides a visual representation of the vibrational modes.

The remaining calculations were performed using the G96LYP functional,[24] which has been recently shown to be one of the more accurate GGA functionals for transition metal-containing systems.[25]

Two different geometries of the $[Cu^{I}(py)_2(OH_2)]^+$ model, with the Cu−O bond either coplanar or perpendicular to the pyridine rings, and a $[Cu^{I}(py)_2(OH_2)_2]^+$ model, constrained to C_{2v} symmetry, were optimized by keeping the Cu−O distance fixed at different values in the 1.9−3.3 Å range, using a triple-ζ valence basis set with polarization functions on all atoms except hydrogen.[26]

For the geometry optimization of the $[CuI(py)_2(SiW_{12}O_{40})]^{3-}$ model the Los Alamos effective core potential combined with a double-ζ basis (LANL2DZ)[27] was chosen for the transition metals, as a compromise between accuracy and computational power available. For the remaining atoms, the D95V basis set[28] was used.

(20) Frisch, M. J.; Trucks, G. W.; Schlegel, H. B.; Scuseria, G. E.; Robb, M. A.; Cheeseman, J. R.; Montgomery, J. A., Jr.; Vreven, T.; Kudin, K. N.; Burant, J. C.; Millam, J. M.; Iyengar, S. S.; Tomasi, J.; Barone, V.; Mennucci, B.; Cossi, M.; Scalmani, G.; Rega, N.; Petersson, G. A.; Nakatsuji, H.; Hada, M.; Ehara, M.; Toyota, K.; Fukuda, R.; Hasegawa, J.; Ishida, M.; Nakajima, T.; Honda, Y.; Kitao, O.; Nakai, H.; Klene, M.; Li, X.; Knox, J. E.; Hratchian, H. P.; Cross, J. B.; Bakken, V.; Adamo, C.; Jaramillo, J.; Gomperts, R.; Stratmann, R. E.; Yazyev, O.; Austin, A. J.; Cammi, R.; Pomelli, C.; Ochterski, J. W.; Ayala, P. Y.; Morokuma, K.; Voth, G. A.; Salvador, P.; Dannenberg, J. J.; Zakrzewski, V. G.; Dapprich, S.; Daniels, A. D.; Strain, M. C.; Farkas, O.; Malick, D. K.; Rabuck, A. D.; Raghavachari, K.; Foresman, J. B.; Ortiz, J. V.; Cui, Q.; Baboul, A. G.; Clifford, S.; Cioslowski, J.; Stefanov, B. B.; Liu, G.; Liashenko, A.; Piskorz, P.; Komaromi, I.; Martin, R. L.; Fox, D. J.; Keith, T.; Al-Laham, M. A.; Peng, C. Y.; Nanayakkara, A.; Challacombe, M.; Gill, P. M. W.; Johnson, B.; Chen, W.; Wong, M. W.; Gonzalez, C.; Pople, J. A. *Gaussian03*; revision C.02; Gaussian, Inc.: Wallingford, CT, 2004.
(21) Reinoso, S.; Vitoria, P.; San Felices, L.; Lezama, L.; Gutiérrez-Zorrilla, J. M. *Chem.—Eur. J.* **2005**, *11*, 1538.
(22) Becke, A. D. *J. Chem. Phys.* **1993**, *98*, 5648.
(23) *Gaussview*, version 3.0; Gaussian, Inc.: Wallingford, CT, 2004.
(24) (a) Lee, C.; Yang, W.; Parr, R. G. *Phys. Rev. B* **1988**, *37*, 785. (b) Gill, P. M. W. *Mol. Phys.* **1996**, *89*, 433.
(25) (a) Schultz, N. E.; Zhao, Y.; Truhlar, D. G. *J. Phys. Chem A* **2005**, *109*, 4388. (b) Schultz, N. E.; Zhao, Y.; Truhlar, D. G. *J. Phys. Chem A* **2005**, *109*, 11127.
(26) Weigend, F.; Ahlrichs, R. *Phys. Chem. Chem. Phys.* **2005**, *7*, 3297.
(27) (a) Hay, P. J.; Wadt, W. R. *J. Chem. Phys.* **1985**, *82*, 270. (b) Wadt, W. R.; Hay, P. J. *J. Chem. Phys.* **1985**, *82*, 284. (c) Hay, P. J.; Wadt, W. R. *J. Chem. Phys.* **1985**, *82*, 299.

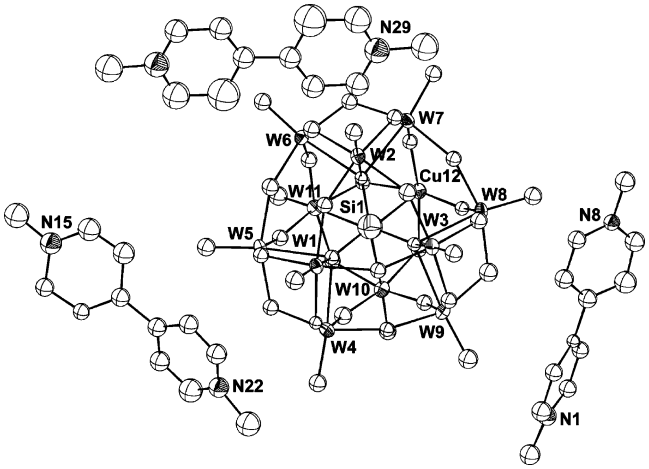

Figure 4. ORTEP view of POM and paraquat cations of compound **2** with tungsten and nitrogen atom labeling.

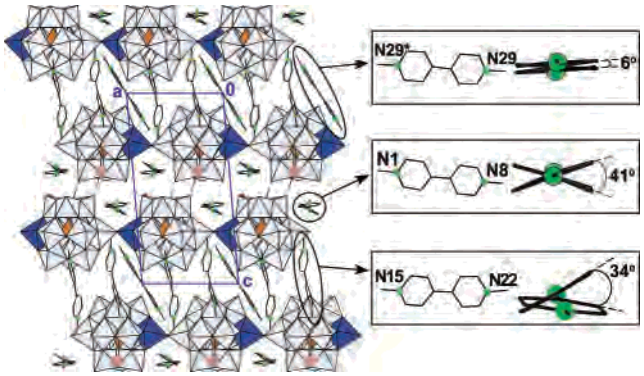

Figure 5. View of the crystal packing of compound **2** along the [010] direction with details of paraquat cations conformation.

Structural Database Survey. The structural data were obtained through a systematic search in the Cambridge Structural Database[29] (CSD version 5.27 updated to Jan 2006) of di-, tri-, and tetracoordinate complexes of Cu(I) bonded to two nitrogens belonging to six-member aromatic rings and with one or two oxygens at a distance shorter than 3.4 Å. Only those structures identified as corresponding to copper oxidation state +1 were retained, and structures which were not error free after CSD evaluation procedures, with reported structural disorder or agreement factors $R >$ 10%, were ruled out.

The CSM calculations of the different Cu(I) polyhedra were performed with the program SHAPE v1.1a.[30]

Results and Discussion

Synthesis and Vibrational Study. When a mixture of $K_8[SiW_{11}O_{39}]\cdot 13H2O$, $CuCl_2\cdot 2H_2O$, oxalic acid dihydrate, and 4,4′-bipyridine in a mixture of methanol and acetic acid/potassium acetate buffer solution reacts under conventional hydrothermal conditions, suitable crystals for X-ray diffraction of cuprite (Cu_2O) and the copper(II)-monosubstituted POM salts **1** and **2** were obtained (Scheme 1). On the other hand, the isolated material from the Teflon reaction vessels in the cases of germanium and phosphorus is mostly compounds **3** and **4**, respectively, mixed with a very small amount of a not yet fully identified compound.

From a preparative point of view, it is interesting to underline the reduction process of copper(II) to copper(I), present in polymeric complexes of compounds **1** and **4.** This reduction process affects only the copper centers forming part of the cationic metalorganic polymers, since the presence of copper(II) ions in the polyanions of all four compounds have been confirmed by single-crystal EPR spectroscopy (see Supporting Information). The N-methylation of bipyridine to give the diquaternary paraquat[31] cation present in compound **2** is also noteworthy. Previous studies describe the N-alkylation of pyridine and 2,4,6-collidine under similar solvothermal conditions, and although the mechanism of the reaction is yet unknown, it has been suggested that the transfer of the alkyl group from the source (methanol or ethanol) takes place only in the presence of oxalate or squarate anions and group 6 metal oxoanions.[32]

The characteristic IR bands of POMs in compounds **1**−**4** and those calculated for the corresponding parent complete $[XW_{12}O_{40}]^{n-}$ Keggin clusters and their copper(II)-monosubstituted derivatives are shown in Table 2. As can be seen, the experimental results are in good agreement with the calculated ones for all the three types of copper(II)-monosubstituted Keggin polyoxotungstates. They give characteristic IR bands in the region 1200−400 cm^{-1},[33] similar to those of the parent $[XW_{11}O_{39}]^{n-}$ monolacunary species due to the fact that both polyanions show the same ideal C_s symmetry. In general, their bands can be observed at wavenumbers between those corresponding to the monolacunary species and those of the complete Keggin cluster, with the exception of the $M-O_a$ antisymmetric stretching (O_a: bridging oxygen atom between edge-sharing MO_6 octahedra), which remains practically constant at ca. 795 cm^{-1} in all the three polyanions. The $\nu_{as}(X-O)$ mode, observed as a single signal in the region 1080−980 cm^{-1} for the parent Keggin POMs, $[XW_{12}O_{40}]^{n-}$ (X: Si, Ge, P), splits in two bands in the spectra of the copper(II)-monosubstituted derivatives, which appear as very weak shoulders of the $\nu_{as}(W-O_t)$ band in the case of the germanium POM. These values correlate very well with the X−O bond distances; thus, the higher $\nu_{as}(X-O)$ values correspond to the shorter X−O bond length. Let us now consider the IR bands in the 750−650 cm^{-1} special region, which involves the $\nu_{as}(Cu-O)$ modes mixed with $\nu_{as}(W-O_a-W)$ bands. These bands are red-shifted as the central heteroatom changes from P to Ge, a fact that is common to all bands in the spectra but especially observed in the mixed bands containing the $\nu_{as}(X-O)$ vibration mode.

(28) Dunning, T. H., Jr.; Hay, P. J. In *Modern Theoretical Chemistry*; Schaefer, H. F., III, Ed.; Plenum: New York, 1976.
(29) Allen, F. H. *Acta Crystallogr.* **2002**, *B58*, 380.
(30) Llunell, M.; Casanova, D.; Cirera, J.; Bofill, J. M.; Alemany, P.; Alvarez, S.; Pinsky, M.; Avnir, D. *SHAPE v1.1a*; Universitat de Barcelona, Spain, 2003.
(31) Summers, L. A. *The Bipyridinium Herbicides*; Academic Press: London, 1980; pp 69−129.
(32) (a) Modec, B.; Brenèiè, J. V.; Dolenc, D.; Zubieta, J. *Dalton Trans.* **2002**, 4582. (b) Modec, B.; Brenèiè, J. V.; Burkholder, E. M.; Zubieta, J. *Dalton Trans.* **2003**, 4618. (c) Modec, B.; Brenèiè, J. V.; Zubieta, J. *Inorg. Chem. Comm.* **2003**, *6*, 506. (d) Modec, B.; Brenèiè, J. V.; Koller, J. *Eur. J. Inorg. Chem.* **2004**, 1611.
(33) Gamelas, J. A. F.; Cavaleiro, A. M. V.; Freire, C.; De Castro, B. *J. Coord. Chem.* **2001**, *54*, 35.

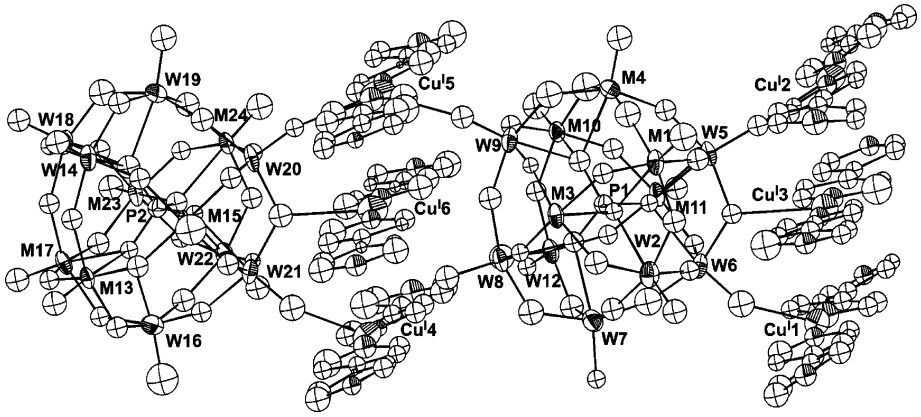

Figure 6. ORTEP view of the two crystallographic independent Keggin POMs and the six copper(I) chains of compound **4** showing their different anchoring to the POMs. M labels mean a significant participation of both copper and tungsten in such a position.

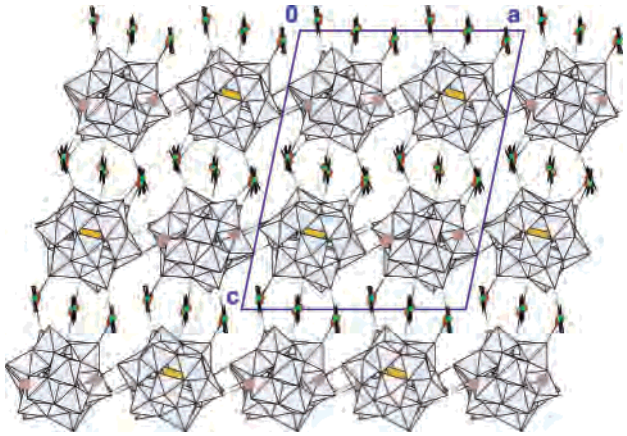

Figure 7. Alternating sequence in compound **4** of inorganic and metalorganic layers, made up of discrete POMs linked by sodium cations and water molecules and stacked copper−bipyridine chains, respectively.

Description of the Crystal Structures. Compounds **1** and **3** are isostructural and crystallize in the orthorhombic space group *Pbcb* with 1 polymeric $[XW_{11}CuO_{39}]^{6-}$ [X: Si (**1**); Ge (**3**)] polyanion, 3 potassium cations, 3 polymeric $[Cu(4,4'\text{-bpy})]^{+}$ cations, and 11 water molecules in the formula unit (Figure 1). Only the crystal structure of compound **1** has been solved due to the low quality of the crystals of compound **3**. The copper-monosubstituted α-Keggin subunit consists of a central SiO_4 tetrahedron surrounded by four vertex-sharing M_3O_{13} trimers: one $Cu^{II}W_2O_{13}$ and three W_3O_{13}. Each Keggin subunit shows two preferential sites for copper(II) atoms at M1 and M7 octahedra with population factors equal to 62 and 38%, respectively. This fact indicates that the bridge between Keggin subunits is always of type $Cu^{II}-O-W$ bridge (Cu1−O1−W7 = 180°), and thus the infinite $[SiW_{11}CuO_{39}]_n^{6n-}$ chain is formed, which lies on a 2-fold axis along the [100] direction. Table 3 displays ranges of W−O bond lengths for compound **1** together with those for the DFT-optimized complete and copper(II)-monosubstituted Keggin POMs.[21]

Compound **1** has a pronounced two-dimensional character and can be viewed as an alternating sequence along the [001] direction of inorganic and metalorganic layers built of mutually perpendicular POM and $[Cu(4,4'\text{-bpy})]_n^{n+}$ chains, respectively (Figure 2). The inorganic sublattice consists of antiparallel POM chains stacked along the crystallographic

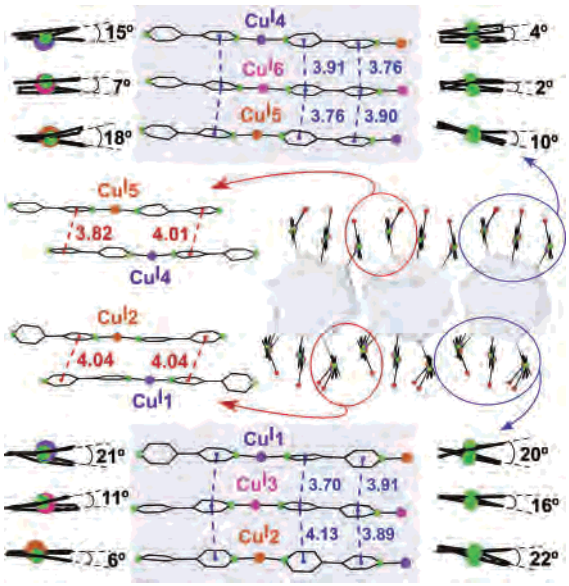

Figure 8. Metalorganic chains in compound **4** with coordination spheres of copper(I) ions and torsion angles between aromatic rings, with details of $\pi-\pi$ interactions along the stacking direction indicating distances between ring centroids.

b axis direction, which are strongly cemented in a two-dimensional arrangement by potassium cations and water molecules. Between inorganic layers chains of copper(I) complexes, running along the *c* axis, are stacked following the [100] direction through the establishment of $\pi-\pi$ interactions between aromatic rings of neighboring chains, with interplanar distances in the range 3.4−3.7 Å (Figure 3). There are two crystallographically independent chains. One of them at $x = 0$, with the $Cu^{I}2$ ions in a N_2O_2 environment showing a N−Cu−N angle equal to 180°, is placed on a binary axis, and it is anchored to the POM through the terminal oxygen atom O6; in contrast, the other chain runs wavy at $x = 1/3$, and the metallic ions ($Cu^{I}1$) are T-shape tricoordinated to two N atoms from 4,4′-bipyridine and the POM bridging oxygen atom O14.

The asymmetric unit of compound **2** contains one $[SiW_{11}CuO_{39}]^{6-}$ subunit, one potassium cation, three paraquat cations, one of them located on a crystallographic inversion center, and six water molecules (Figure 4). The inorganic sublattice is made up of POM double chains, each formed

Table 4. Selected Bond Distances (Å) and Angles (deg) of the Cu(I) Coordination Spheres in Compounds **1** and **4**[a,b]

Compound **1**

Cu^I1		Cu^I2	
Cu^I1-N1	1.89(3)	Cu^I2-N13	1.85(3)
Cu^I1-N7	1.88(2)	Cu^I2-N20	1.86(4)
Cu^I1-O14	2.75(2)	Cu^I2-O6	2.88(2)
		Cu^I2-O6^i	2.88(2)
$N1-Cu^I1-N7$	167.4(9)	$N13-Cu^I2-N20$	180.0(1)
$N1-Cu^I1-O14$	97.7(9)	$N13-Cu^I2-O6$	88.2(4)
$N7-Cu^I1-O14$	94.9(9)	$N13-Cu^I2-O6^i$	88.2(4)
		$N20-Cu^I2-O6$	91.9(4)
		$N20-Cu^I2-O6^i$	91.9(4)
intra-$Cu^I1\cdots Cu^I1^{ii}$	10.900(5)	$Cu^I2\cdots Cu^I2^{ii}$	10.798(6)
inter-$Cu^I1\cdots Cu^I2$	3.756(4)		

Compound **4**

Cu^I1		Cu^I2		Cu^I3	
Cu1−N1	1.90(2)	Cu^I2-N8	1.89(3)	Cu^I3-N55	1.84(2)
Cu^I1-N25	1.94(3)	Cu^I2-N33	1.91(2)	Cu^I3-N49	1.89(2)
Cu^I1-O6	2.36(3)	Cu^I2-O18	2.62(2)	Cu^I3-O35	2.84(2)
		Cu^I2-O5^{iii}	2.67(2)		
$N1-Cu^I1-N25$	171(1)	$N8-Cu^I2-N33$	171(1)	$N55-Cu^I3-N49$	172(1)
$N1-Cu^I1-O6$	90(1)	$N8-Cu^I2-O18$	88(1)	$N55-Cu^I3-O35$	91(1)
$N25-Cu^I1-O6$	97(1)	$N8-Cu^I2-O5^{iii}$	91(1)	$N49-Cu^I3-O35$	92(1)
		$N33-Cu^I2-O18$	95(1)		
		$N33-Cu^I2-O5^{iii}$	94(1)		
intra-$Cu^I1\cdots Cu^I2$	10.908(6)			$Cu^I3\cdots Cu^I3^{iv}$	10.912(6)
inter-$Cu^I1\cdots Cu^I3$	3.60(1)	$Cu^I2\cdot\cdot Cu^I3^{iii}$	3.94(3)		

Cu^I4		Cu^I5		Cu^I6	
Cu^I4-N20	1.92(2)	Cu^I5-N13	1.89(3)	Cu^I6-N69	1.88(2)
Cu^I4-N40	1.92(3)	Cu^I5-N37	1.96(2)	Cu^I6-N61	1.97(2)
Cu^I4-O21	2.41(3)	Cu^I5-O9	2.66(2)	Cu^I6-O66	2.81(3)
		Cu^I5-O20^{iv}	2.77(2)		
$N20-Cu^I4-N40$	170(1)	$N13-Cu^I5-N37$	175(1)	$N69-Cu^I6-N61$	174(1)
$N20-Cu^I4-O21$	98(1)	$N13-Cu^I5-O9$	92(1)	$N69-Cu^I6-O66$	94(1)
$N40-Cu^I4-O21$	92(1)	$N13-Cu^I5-O20^{iv}$	93(1)	$N61-Cu^I6-O66$	92(1)
		$N37-Cu^I5-O9$	91(1)		
		$N37-Cu^I5-O20^{iv}$	87(1)		
intra-$Cu^I4\cdots Cu^I5$	10.908(6)			$Cu^I6\cdots Cu^I6^{iii}$	10.908(6)
inter-$Cu^I4\cdots Cu^I6$	3.80(1)	$Cu^I5\cdots Cu^I6^{iv}$	3.65(1)		

[a] Symmetry codes: (i) $2-x, y, {}^1/_2-z$; (ii) $x, -{}^1/_2+y, {}^1/_2-z$; (iii) ${}^1/_2-x, {}^1/_2+y, 1-z$; (iv) ${}^1/_2-x, -{}^1/_2+y, -z$. [b] Intra: nearest intrachain Cu···Cu distance. Inter: nearest interchain Cu···Cu distance.

by two antiparallel $[SiW_{11}CuO_{39}]_n^{6n-}$ polymeric polyanions linked through the coordination sphere of K1 cations, stacked along the [010] direction (Figure 5). This two-dimensional inorganic arrangement generates a region at $z = 0$ where two-thirds of the paraquat cations are placed in such a way that the methyl groups penetrate into the POM chains to establish C−H···O contacts that link adjacent inorganic shells. On the other hand, the remaining diquaternary cations are buried inside the hexagonal channels formed along the stacking direction of the POM double chains, reinforcing the inorganic sublattice through hydrogen contacts involving the methyl hydrogen atoms, POM oxygens, and water molecules.

Compound **4** contains two discrete $[PW_{11}CuO_{39}(H_2O)]^{5-}$ Keggin polyanions, six polymeric $[Cu(4,4'\text{-bpy})]^+$ cations, four sodium cations, and eight water molecules in the asymmetrical unit (Figure 6). This compound, just like **1**, has a two-dimensional character formed by an alternating sequence along the crystallographic *c* axis of inorganic (at $z = 1/4, 3/4$) and metalorganic (at $z = 0, 1/2$) layers (Figure 7). In the inorganic sublattice the discrete Keggin POMs are strongly bound by sodium cations and water molecules in an extensive hydrogen bond network. The two crystallographically independent metalorganic layers are made of polymeric $[Cu(4,4\text{-bpy})]_n^{n+}$ complex cations running parallel to the *b* axis and stacked along the [100] direction forming triads of chains. The 4,4′-bipyridine ligands inside these triads arrange in a nearly parallel fashion, and they are involved in intermolecular $\pi-\pi$ interactions with average interplanar and intercentroidal distances of 3.6 and 3.9 Å, respectively (Figure 8). The coordination number of the copper(I) ions ranges from 2 to 4, being the third and fourth positions occupied by either terminal or bridging POM oxygen atoms. In this way, each POM is coordinated or semicoordinated to four copper ions, which bridge POMs belonging to adjacent inorganic shells.

Copper(I) Coordination Spheres. Copper(I) atoms in the polymeric bipyridine cationic complexes present a nearly linear coordination to the nitrogen atoms, so they can easily accommodate one or two POM surface oxygen atoms giving 2 + 1 (Cu1 for compound **1** and Cu1, Cu3, Cu4, and Cu6 for compound **4**) or 2 + 2 (Cu2 for compound **1** and Cu2 and Cu5 for compound **4**) distorted geometries. As can be seen in Table 4 the Cu−N bond distances remain almost constant (1.84−1.97 Å), whereas the Cu−O distances present

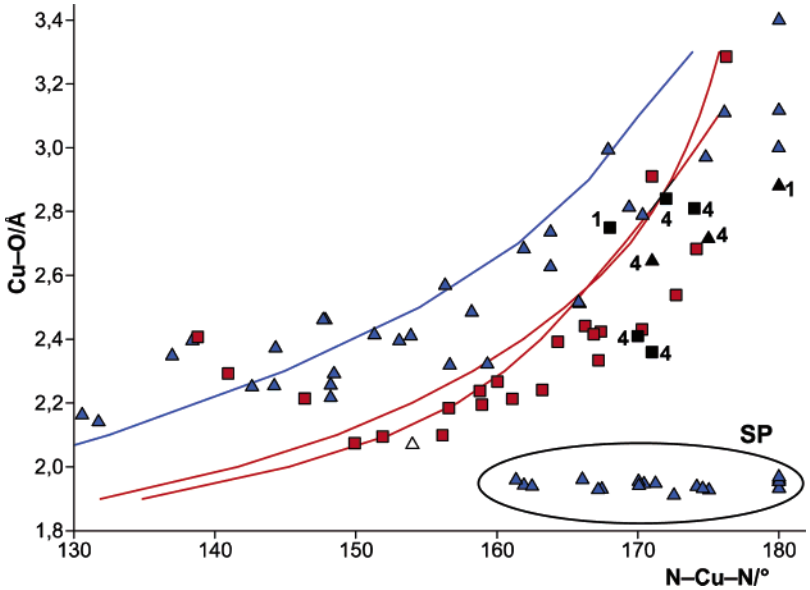

Figure 9. Correlation between the N−Cu−N bond angle and the Cu−O distance (average value for CuN_2O_2 complexes) for CuN_2O tricoordinated (triangles) and CuN_2O_2 tetracoordinated (squares) Cu(I) complexes, either retrieved from the CSD database (blue and red symbols), from compounds **1** and **4** (black symbols with numerical label), or from DFT calculations of $[Cu(py)_2(OH_2)]^+$ (red lines), $[Cu(py)_2(OH_2)_2]^+$ (blue line), and $[Cu(py)_2(SiW_{12}O_{40})]^{3-}$ (empty triangle) models.

Table 5. Continuous Shape Measures of the Cu(I) Coordination Spheres in Compounds **1** and **4**[a]

	1		**4**					
CSM	Cu^I1	Cu^I2	Cu^I1	Cu^I2	Cu^I3	Cu^I4	Cu^I5	Cu^I6
TP, D_{3h}	3.72		5.28		5.17	4.58		4.62
VT, C_{3v}	6.40		7.18		7.69	7.18		7.11
SP, D_{4h}		4.55		12.87			6.89	
T, T_d		36.33		9.66			17.54	
SW, C_{2v}		16.86		6.48			8.97	

[a] CSM: continuous shape measures. TP: trigonal planar. VT: pyramid (vacant tetrahedron). SP: square. T: tetrahedron. SW: sawhorse (cis-divacant octahedron).

a wide variation in the range 2.36−2.88 Å. Moreover, the N−Cu−N bond angle deviates only slightly from linearity independently of the corresponding Cu−O bond distance. As the d^{10} ions of the group 11 show variable and ambiguously defined coordination numbers,[34] a search of the CSD database has been carried out to obtain some insights on the preferred geometries around the copper(I) atoms coordinated both to N-heterocycles and O-donor ligands. The different Cu(I) coordination spheres of compounds **1** and **4** and those retrieved from the CSD database have been characterized by employing continuous shape measures (CSM),[9c,35] which determine the normalized distance of a structure from a given reference shape: trigonal planar(TP) or pyramidal (VT) and sawhorse (SW), tetrahedron (T), or square planar (SP) for tri- and tetracoordinated complexes, respectively.

As can be seen in Figure 9, the N−Cu−N angle shows a continuous distribution between 130 and 180°. Although there is some scatter mainly due to the variable nature and denticity of the ligands, especially the O-donors, which range from neutral water molecules to nitrate or carboxylate anions, the N−Cu−N angle and the Cu−O distance are inversely correlated: the departure from linearity is larger as the ligands get closer to the Cu(I) atom. The group of structures at the bottom right corner of the graph that do not follow this trend, with the shortest Cu−O distances, are all slightly distorted square planar (SP) complexes, as seen by inspection and because they show a very small CSM with respect to the ideal square planar geometry, $0.0 < S(SP) < 1.3$. In fact, the other structures have large CSMs with respect to any reference shape, which means that they are heavily distorted, a fact also observed for the Cu(I) coordination spheres present in compounds **1** and **4** (Table 5 and Supporting Information).

The DFT optimizations of the $[Cu(py)_2(OH_2)]^+$ and $[Cu(py)_2(OH_2)_2]^+$ models at fixed Cu−O distances display a correlation similar to that found experimentally and also show that, for a fixed mean Cu−O distance, the tetracoordinated model has quite a smaller N−Cu−N angle than the tricoordinated one, as it tends toward a tetrahedral instead of a trigonal planar geometry. This fact also appears in the experimental distribution, albeit not so clearly due to the scatter.

Besides, in all models the calculated potential energy surface for N−Cu−N bending is very flat, since all structures with a N−Cu−N angle in the 130−180° range are in a 7

(34) Carvajal, M. A.; Novoa, J. J.; Alvarez, S. *J. Am. Chem. Soc.* **2004**, *126*, 1465.
(35) (a) Zabrodsky, H.; Peleg, S.; Avnir, D. *J. Am. Chem. Soc.* **1992**, *114*, 7843. (b) Alvarez, S.; Llunell, M. *J. Chem. Soc., Dalton Trans.* **2000**, 3288. (c) Alvarez, S.; Avnir, D.; Llunell, M.; Pinsky, M. *New J. Chem.* **2002**, *26*, 996. (e) Alvarez, S. *Anal. Quim.* **2003**, *99*, 29.

kcal/mol envelope. This shallowness of the potential energy surface agrees nicely with the large distortions from ideal geometries and the continuous distribution in Figure 9 and shows that the shape and geometrical details of a particular Cu(I) coordination sphere must be highly dependent on the nature of the O-donor ligand and crystal packing details. In fact, the DFT-optimized $[Cu(py)_2(SiW_{12}O_{40})]^{3-}$ molecule has a shorter Cu−O bond (2.07 Å) and thus a smaller N−Cu−N angle (154°) than those found in compounds **1** and **4**. This must be due to a stronger interaction between the Keggin anion and the complex cation, which leads to quite short C−H···O hydrogen bonds, because the calculation is in the gas phase and the multiple intermolecular interactions present in the crystals are missing.

Conclusions

We have synthesized and structurally characterized four new inorganic−metalorganic hybrid compounds. From a synthetic point of view, the presence of copper(I) in compounds **1**, **3**, and **4** and of the paraquat diquaternary cation in compound **2** together with the formation of cuprite as a byproduct is quite noteworthy and due to the reduction process of copper(II) to copper(I) and the N-methylation of bipyridine under hydrothermal conditions.

The crystal packings are characterized by the presence of monodimensional extended entities: either the polymeric polyanion $[SiW_{11}Cu^{II}O_{39}]_n^{6n-}$ (**2**), $[Cu^{I}(4,4'\text{-bpy})]_n^{n+}$ chains (**4**), or, which is noteworthy, both simultaneously as in compound **1**, where the inorganic and metalorganic sublattices are mutually perpendicular.

The considerable structural variation at the copper(I) sites of compounds **1**, **3**, and **4** has been analyzed using the CSD database and DFT calculations, which have shown that the shape and geometrical details of a particular Cu(I) coordination sphere are highly dependent on the nature of the O-donor ligand and crystal packing details, since the potential energy surface for N−Cu−N bending is quite flat.

Acknowledgment. This work was supported by Universidad del País Vasco (Grant 9/UPV00169.310-15329/2003) and Ministerio de Ciencia y Tecnología (Grant MAT2005-03047). L.S.F. thanks Ministerio de Ciencia y Tecnología for her Doctoral Fellowship. Computational resources were provided by the SGI/IZO-SGIker at the UPV/EHU (supported by the Spanish Ministry of Education and Science and the European Social Fund).

Supporting Information Available: Figures showing the Q-band single-crystal EPR spectrum of compound **1** and DFT calculated infrared spectra of the parent and copper(II)-monosubstituted Keggin anions, listings of continuous symmetry measures (CSM) for all entries retrieved from the CSD database, and X-ray crystallographic files of compounds **1**, **2**, and **4** in CIF format. This material is available free of charge via the Internet at http://pubs.acs.org.

IC060762G